

## Article

# Diagenesis of the Permian Fengcheng Formation in the Mahu Sag, Junggar Basin, China

Bin Bai <sup>1,\*</sup>, Jiwei Liang <sup>2</sup>, Chaocheng Dai <sup>3</sup>, Wenjun He <sup>4</sup>, Ying Bai <sup>1</sup>, Xiaobin Chang <sup>2</sup>, Meng Zheng <sup>2</sup>, Hanlin Li <sup>2</sup> and Hao Zong <sup>2</sup>

<sup>1</sup> Research Institute of Petroleum Exploration & Development, Beijing 100083, China; byshimmer@petrochina.com.cn

<sup>2</sup> School of Earth Sciences and Resources, Chang'an University, Xi'an 710054, China; jiweil@chd.edu.cn (J.L.); 2020127045@chd.edu.cn (X.C.); 2021127054@chd.edu.cn (M.Z.); zjie47365@gmail.com (H.L.); m15191857101@163.com (H.Z.)

<sup>3</sup> School of Earth Sciences, East China University of Technology, Nanchang 330013, China; daichaocheng@ecut.edu.cn

<sup>4</sup> Research Institute of Exploration and Development, Xinjiang Oilfield Company, PetroChina, Karamay 834000, China; fchwj@petrochina.com.cn

\* Correspondence: baibin81@petrochina.com.cn

**Abstract:** The Fengcheng Formation in the Mahu sag of the Junggar Basin was primarily composed of detritus, pyroclastic material, carbonates, and evaporites. In order to establish the diagenesis pathways of the Fengcheng Formation, some methods of polarized light microscope, SEM, CL, EPMA, LR, and fluid inclusion analysis were applied to discuss the diagenesis process. The results showed the following: (a) The formation of an alkaline lake was the result of the influence of a high concentration of sodium-rich sources, and it led to the preservation of alkaline minerals in the stratum. (b) After the sediments were buried, three mineral assemblages were formed in the Fengcheng Formation, which are carbonate mineral assemblages (i.e., calcite + ferrous dolomite), reedmergnerite and carbonate mineral assemblages (i.e., reedmergnerite + calcite + ferrous dolomite), and reedmergnerite and alkaline mineral assemblages (i.e., reedmergnerite + shortite + trona), respectively. (c) According to the homogenization temperature of reedmergnerite primary fluid inclusions, the alkaline diagenesis of Fengcheng Formation was divided into an early stage ( $\leq 100$  °C) and a middle stage ( $> 100$  °C), respectively. The earlier stage is marked by the formation of ferrous saddle dolomite, quartz dissolution, and the agglutination of laumontite. These processes occurred under normal burial conditions. The latter is marked by the reedmergnerite's appearance, which is correlated with the deep hydrothermal activity controlled by faults. (d) Based on sedimentary and diagenetic factors, including climate, provenance, diagenetic surroundings, and the action of subsurface fluid, the alkaline deposition-diagenesis model for shale series in four stages of the Fengcheng Formation was established.

**Keywords:** diagenesis pathways; Fengcheng Formation; Mahu sag; northwest China



**Citation:** Bai, B.; Liang, J.; Dai, C.; He, W.; Bai, Y.; Chang, X.; Zheng, M.; Li, H.; Zong, H. Diagenesis of the Permian Fengcheng Formation in the Mahu Sag, Junggar Basin, China. *Appl. Sci.* **2023**, *13*, 13186. <https://doi.org/10.3390/app132413186>

Academic Editor: Fabrizio Balsamo

Received: 19 October 2023

Revised: 15 November 2023

Accepted: 29 November 2023

Published: 12 December 2023



**Copyright:** © 2023 by the authors. Licensee MDPI, Basel, Switzerland. This article is an open access article distributed under the terms and conditions of the Creative Commons Attribution (CC BY) license (<https://creativecommons.org/licenses/by/4.0/>).

## 1. Introduction

Traditional early and middle diagenesis is mainly conducted in acidic diagenetic environments, which are characterized by carbonate mineral, feldspar, and clay minerals being in an unstable state and easy to be dissolved [1–5]. When the reservoir experiences an alkaline diagenetic environment, reservoir property is often changed due to the role of alkaline formation water, quartz dissolution, feldspar enlargement, and carbonate mineral replacement becoming the most distinctive diagenetic phenomena [6–11]. The theory of alkaline diagenesis has enriched, improved, and deepened the traditional theory of diagenesis. At present, the understanding of alkaline diagenesis is relatively insufficient compared to traditional diagenesis. The conditions of alkaline diagenesis generally include

a sedimentary environment, climate, organic acids, and thermal fluid evolution [12,13]. Alkaline diagenesis can have constructive effects on reservoirs [14,15]. For example, mica interlaminar pores and albite pores formed under the action of alkaline fluids are good oil storage spaces. The diagenetic phenomena of alkaline diagenesis are diverse, including alkali lacustrine salt rocks [16], alkaline evaporative salt minerals [17], and quartz dissolution under the action of alkaline groundwater [18]. In addition, alkaline diagenesis may also provide a new explanation for the silicification of metal deposits, the origin of siliceous cementation, and the reddening and fragmentation of rocks [11–19].

The Junggar Basin is located in northwestern China (Figure 1a), with an area of about 1393 square kilometers [20]. The basin is divided into six first-level structural units: Ulungu sag, Luliang uplift, Western uplift, Central sag, Eastern uplift, and North Tianshan thrust band [21] (Figure 1a). The Mahu sag, located northwest of the Central sag of the Junggar Basin in an NE trend, is the most petroliferous sag (Figure 1). The most important source rock in the northwestern part of the Mahu sag is the lower Permian Fengcheng Formation [3,21,22]. The Fengcheng Formation consists of a mixed shale series comprising carbonate rocks, alkaline intermediate to basic volcanic rocks, and terrigenous detrital rocks. It contains alkaline minerals such as kanemite, bradleyite, and eitelite, suggesting formation in an alkaline lake environment [23]. The rocks of the Fengcheng Formation also contain bands and clumps of the uncommon mineral reedmergnerite [Na(BSi<sub>3</sub>O<sub>8</sub>)], indicating that it has undergone complex diagenetic processes [4–6]. The Fengcheng Formation is a fair-to-good source rock development horizon with high organic matter content, which has the characteristics of multi-phase hydrocarbon generation peak and large-area hydrocarbon generation [23,24]. Meanwhile, the Fengcheng Formation has good exploration prospects and development value for oil and gas exploration, which has been widely concerned in the oil field recently. Studies show that the alkali lake of the Fengcheng Formation has experienced five stages of drought-wet-dry-heat-continuous dry-heat-humid [25], forming major reservoir types, including dolomite, clastic rock, and volcanic rock, and the formation of alkaline minerals is closely related to the evaporative salinization of lake brine [26]. The study of the alkaline lake environment and its diagenesis is still in the initial stage and needs to be further studied. Focused on the Fengcheng Formation, this study tried to obtain (1) the petrological and mineralogical characteristics, (2) diagenetic types, (3) and sedimentary diagenetic models, and this study is helpful for promoting the theoretical innovation of the Fengcheng Formation for further oil and gas exploration purposes.

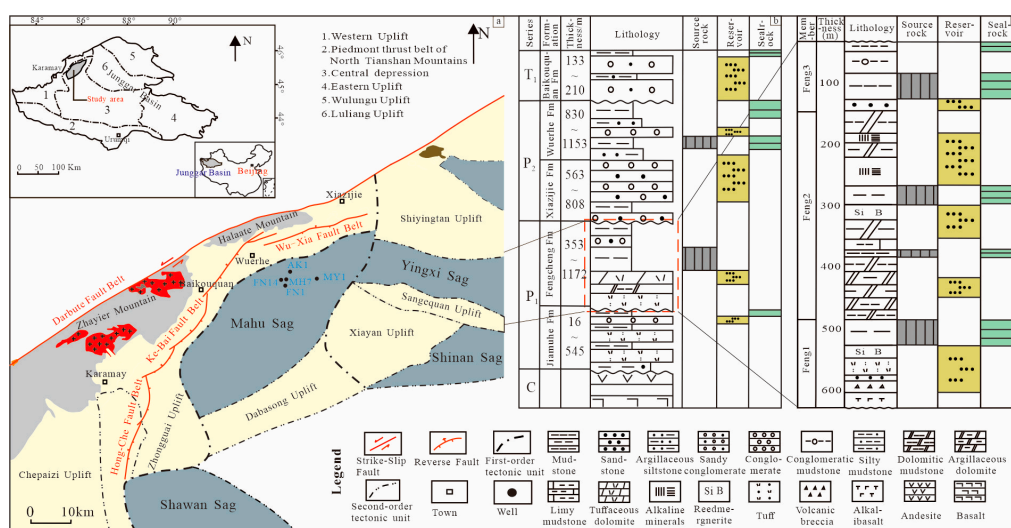


**Figure 1.** Tectonic and lithofacies paleogeographic maps of the Mahu Depression in the Junggar Basin: (a) map of tectonic units in the Mahu Depression, Junggar Basin (with well location) (adapted from [14,27]); (b) lithologic columns of the Permian and Fengcheng Formation in the Mahu Depression (adapted from [26]); (c) source-reservoir-cap assemblage diagram (taking well FN1 as an example).

## 2. Geological Setting and Samples

The northeastern part of the Junggar Basin is close to the Qingridi Mountains and Kelamei Mountains, the southern part is adjacent to the Tianshan Mountains, and the northwest/western parts are the Delun Mountains, Halaalate Mountains, and Zaire Mountains, which are nearly triangular, with a sharp southeast and a wide northwest (Figure 1a). The Junggar Basin, an important part of the Central Asian Orogenic Belt [21], belongs to the superimposed basin [28,29], whose Late Devonian/Early Carboniferous contribution was rift basins, while the Late Carboniferous/Permian period formed foreland basins, and the Triassic/Paleogene periods formed intracontinental depression basins [27]. From the Early Paleozoic to the end of the Late Paleozoic Carboniferous period, the Junggar Basin had a long-term multi-island oceanic paleogeographic pattern with discrete island arcs and ocean basins arranged alternately [28], and with the evolution of the Paleo-Asian Ocean Basin, the marine area gradually diminished [28]. When the Jiamuhe Formation was deposited in the Early Permian period, some areas in the basin evolved into residual marine facies [30], until the Early Permian Fengcheng Formation. During this period, the Fengcheng, Wuerhe, and Xiazijie areas in the Mahu sag evolved into salinized lake basin facies after the closure of the residual sea [25].

The Mahu sag is located in the northwest part of the Central sag of the Junggar Basin in an NE trend. It is a secondary structural unit in the basin [28], with a length of about 100 km, a width of about 50 km, and an area of about 5000 square kilometers [30]. The tectonic unit dips gently to the southeast as a whole [31] and is one of the sags with the richest oil and gas content in the basin [32,33]. The Mahu sag is adjacent to the Kebai and Wuxia large fault zones in the northwest [34], the Yingxi sag in the east, the Dabasong-Xiayan uplift in the southeast, and the Zhongguai uplift in the southwest [25,35] (Figure 1a), and it was developed on the pre-Carboniferous folded basement [27]. The Lower Permian Fengcheng Formation is the main source of rock formation in the Mahu sag [36], with a maximum formation thickness of 1500 m [26]. It is the oldest alkali lacustrine source rock discovered in the world so far [37]. It experienced three periods of hydrocarbon generation peaks: Late Permian, Late Triassic, and Late Cretaceous [29], and the generated oil and gas were accumulated in the Fengcheng Formation and its overlying Wuerhe Formation and Baikouquan Formation [38]. According to the rock combination, from bottom to top, the Fengcheng Formation can be divided into three sections, including Feng 1, Feng 2, and Feng 3. The Feng 1 Member mainly develops volcanic rocks, the Feng 2 Member develops mudstone and carbonate rocks, which are rich in reedmergnerite, and the Feng 3 Member mainly develops terrigenous detrital rocks (Figure 1b,c).

## 3. Analytical Methods

Castings and multi-purpose slices of exploratory well cores such as FN1, FN14, AK-1, and MH7 are used as the main experimental objects.

### 3.1. Morphology and Microscopic Features Analyses

The multi-purpose and cast thin sections were analyzed by a polarized light microscope to obtain key information such as the type, morphology, and mutual relationship between minerals in thin sections, and the pores were observed. At the same time, the microscopic features of minerals such as quartz, zeolite, and clay were recorded under the scanning electron microscope (SEM), and the ring-band structure of carbonate minerals was observed in the cathode luminescence (CL) test. The scanning electron microscope (SEM-QUANTA650, FEI Co., USA) experiment was completed in the Mineralization and Dynamics Laboratory of Chang'an University, and the cathode luminescence (CL 8200mk5-2, Germany) test was carried out in the Xi'an National Engineering Laboratory for Low Permeability Oil and Gas Field Exploration and Development.

### 3.2. Compositions of Minerals Analyses

For Mg-Ca carbonate minerals and special alkaline minerals widely distributed in thin slices, electron probe microanalysis (EPMA) was used to determine the composition of carbonate minerals, to determine the specific content of each component, and to assist in determining the type of alkaline minerals. Because the reedmergnerite in alkaline minerals is special, the laser Raman method (LR) was used to analyze it. The LinkamTHMS600 (Britain) geological cold and hot platform was used for testing the homogenization temperature of reedmergnerite primary fluid inclusions. The electron probe (EPMA-JXA8100, Jeol, Japan) experiment was completed in the Mineralization and Dynamics Laboratory of Chang'an University, and the laser Raman (Renishaw in Via type confocal laser Raman spectrometer, Britain) test experiment was completed in the Xi'an Institute of Geology and Mineral Resources.

In order to avoid the interference of external substances and assure the accuracy of the experimental results, all core slices were stored in slice boxes before the experiment, and the experimental process was strictly operated according to the standard [4–8].

## 4. Results

### 4.1. Petrological Characteristics

The Fengcheng Formation is a set of mixed shale series composed of alkaline intermediate-basic volcanic rocks, carbonate rocks, and terrigenous clastic rocks.

#### 4.1.1. Volcanic Rock

Volcanic rocks are one of the rock types in the study area, which were mainly developed in the Fengcheng 1 Member, and they can be divided into three categories: subvolcanics, volcanic lava, and volcanic clastic rocks (Figure 2). Subvolcanics are also divided into basaltic porphyrite and esitic porphyrite. Basalt, andesitic rock, and trachyte could be determined from volcanic lava. Volcanic clastic rocks mainly consist of tuff and breccia. Rock and mineral identification and previous studies showed that the volcanic rocks are mainly intermediate-basic. The discovery of the silica-alkali diagram and titan pyroxene (Table 1) of volcanic rocks showed that the volcanic rocks of the Fengcheng Formation are alkaline.

**Table 1.** EPMA data table of titanagite and iron dolomite (wt.%).

	Na <sub>2</sub> O	TiO <sub>2</sub>	SO <sub>3</sub>	SiO <sub>2</sub>	FeO	P <sub>2</sub> O <sub>5</sub>	Al <sub>2</sub> O <sub>3</sub>	MnO	K <sub>2</sub> O	MgO	BaO	CaO	Total
	0.07	0.22	-	-	9.39	-	0.01	0.46	0.01	15.49	0.09	27.91	53.65
	-	-	-	0.03	9.38	0.06	0.02	0.62	0.02	15.01	-	27.85	52.99
	-	-	0.06	-	8.01	-	-	0.11	0.01	17.58	-	30.84	56.61
	-	-	-	-	6.44	0.02	0.02	0.37	-	17.99	0.09	32.02	56.95
Iron	-	0.04	0.04	0.01	12.99	-	0.05	0.33	-	13.96	-	29.45	56.87
dolomite	-	-	0.04	-	10.98	0.04	0.01	0.54	0.01	13.74	0.07	28.03	53.46
	-	-	-	0.16	6.69	-	0.08	0.18	0.03	17.85	0.04	31.10	56.13
	-	-	0.04	-	8.41	0.01	-	1.21	0.04	18.25	-	32.05	60.01
	-	0.05	-	-	7.45	0.01	-	0.86	-	17.49	0.13	30.46	56.45
	0.07	0.08	0.25	8.54	5.43	0.08	1.86	0.16	0.54	15.58	-	23.58	56.17
Titanagite	0.024	20.276	0.056	37.513	8.687	0.051	6.745	0.122	0.116	2.243	0.073	18.156	94.06

#### 4.1.2. Carbonate Rocks

Carbonate rocks are mainly dolostone and argillaceous dolomite developed in the second member of the Fengcheng Formation, while only thin or small carbonate lenses are found in the Fengcheng 1 Member and the Fengcheng 3 Member (Figure 1b,c). The middle striation of dolomite is developed, and most is interbedded with argillaceous rocks. Dolomites are mostly fine-grained with microcrystalline clays, and the content of dolomite is 45–65 wt.% (atomic percent). A small amount of volcanic tuff, including volcanic eruptions and terrigenous, fine-grained tuff debris, is visible in some dolomites [39].

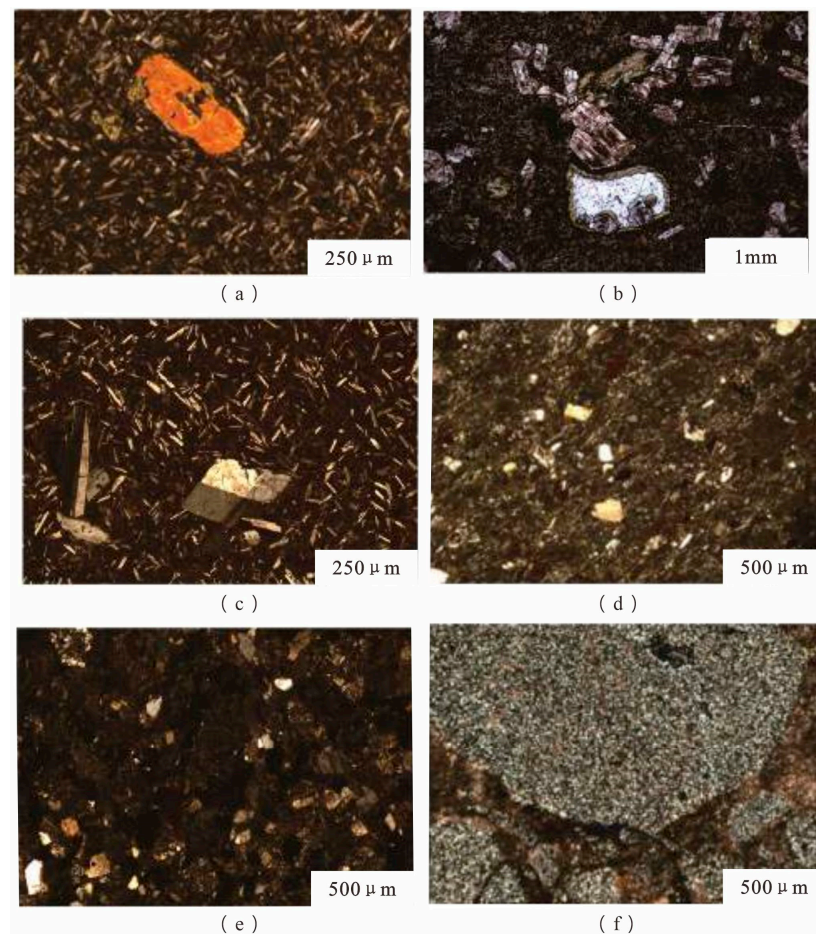


**Figure 2.** Petrological characteristics of volcanic rocks in the Mahu Depression. Subvolcanics: (a) basaltic porphyrite; (b) andesitic porphyrite and volcanic lava; (c) basal; (d) trachyte and volcanic clastic rocks; (e) tuff; (f) tuff breccia.

#### 4.1.3. Terrigenous Clastic Rocks

The terrigenous clastic rocks are conglomerate, sandstone, and mudstone. Conglomerate and sandstone are developed in the Fengcheng 3 Member. Dolomite particles and volcanic tuff are common in the rocks. The closer the lake basin edge is, the larger the particle size is, and the debris may mainly come from the Zaire Mountain in the west of the Mahu sag [40,41]. Mudstone is very common in the Feng 1, Feng 2, and Feng 3 sections. The thickness of Feng 2 is large, and it is rich in bacteria and organic algae matter [26,28]. It is the main source rock position of the Fengcheng Formation. There are seasonal laminae [40–42]. Microcrystalline calcite, in some areas of mudstone, experienced dolomitization and transformed to dolomite, with lake water as the Mg source.

#### 4.2. Mineralogical Characteristics

Fe-bearing dolomite, calcite, and other minerals are significant diagenetic components of the shale series in the Fengcheng Formation within the Mahu sag. Studying the relationship between them is of great significance for the classification of alkaline diagenesis. The Fengcheng Formation in this area is preliminarily divided into three mineral assemblages: carbonate mineral assemblage, borosilicate-carbonate mineral assemblage, and borosilicate-alkaline mineral assemblage.

The dolomite of the Fengcheng Formation generally contains iron (Table 1), with the highest iron content of 13% and an average of 8.5% [43].  $\text{Fe}^{2+}$  does not replace half of  $\text{Mg}^{2+}$ ; thus, it is iron dolomite. There are three forms of iron dolomite: mud microcrystal layered (Figure 3a), powder crystal block (Figure 3b,c), and snowflake (Figure 3d,e). Under

cathode luminescence, the band structure of mud-microcrystalline layered iron dolomite is only occasionally seen. The fine-grained block and snowflake-like iron dolomites have a clear ring structure, which can be divided into irregular undulate type I ring combination (Figure 3e) and rhombic type II ring combination (Figure 3f). The edge morphology of the outermost ring of the type II ring combination is different, mostly in a straight shape (Figure 3f), and occasionally in a serrated or clamshell shape, which may be caused by late corrosion events [35,36]. It is difficult to see pure calcite in the Fengcheng Formation. Calcite has been replaced by dolomite or iron dolomite, and a small part has been replaced by sodium borosilicate (Figure 3g). Reedmergnerite [Na(BSi<sub>3</sub>O<sub>8</sub>)] is a rare diagenetic mineral, mainly distributed in the Feng 1 and Feng 2 Members, and it often coexists with carbonate minerals. After calcite dolomitization, iron dolomite was replaced by borosilicate; some reedmergnerite developed metasomatic relict texture, and carbonate minerals remained in the minerals (Figure 3h). It is inferred that the formation age of borosilicate is later than that of carbonate minerals. The reedmergnerite can be divided into two types according to the degree of self-shape: wedge-shaped reedmergnerite with a high degree of self-shape and diamond-plate-shaped reedmergnerite with a low degree of self-shape (Figure 4b) and wreck-shaped reedmergnerite (Figure 3h). The former is mostly aggregated growth (Figure 4a), while the latter is mostly scattered in the matrix. The mineral is not pure inside, and the mineral edge is jagged or irregularly radial.

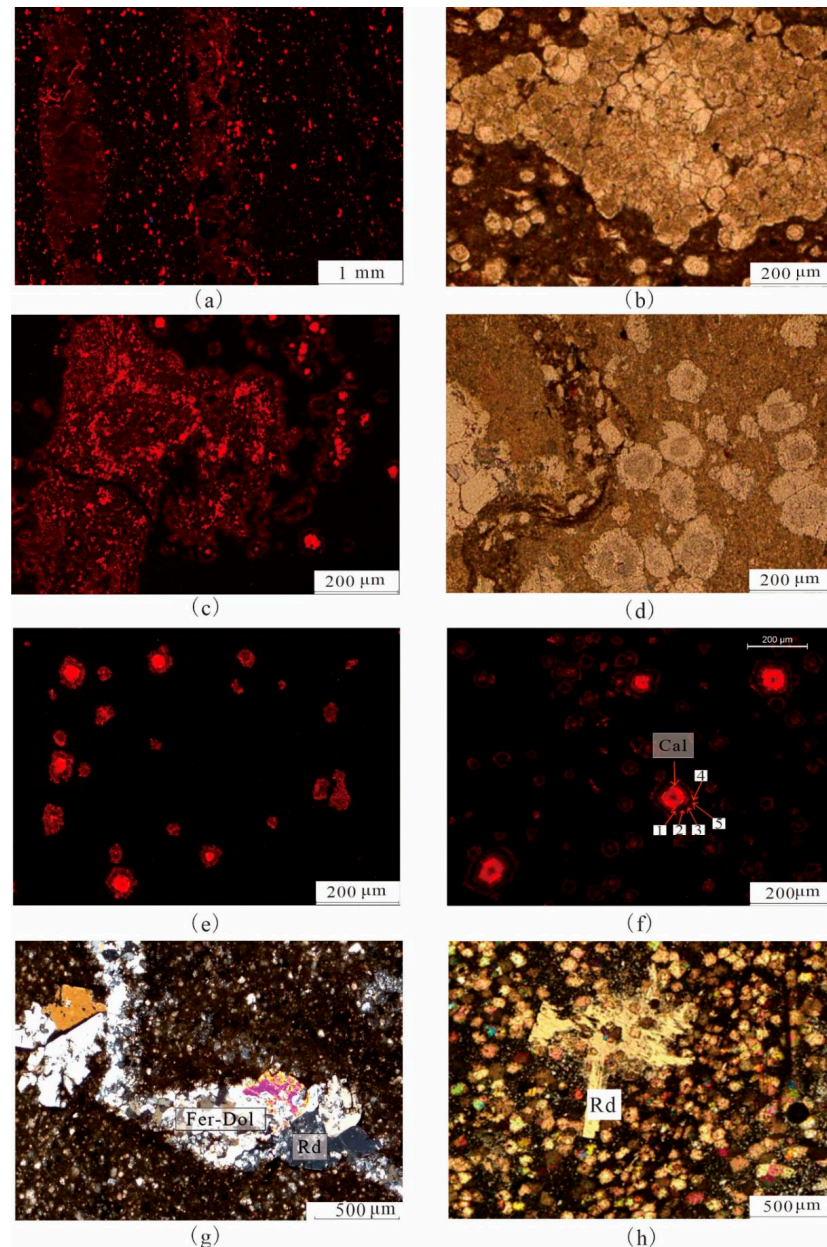
Under the microscope, the butterfly-shaped twinned crystals and a group of complete cleavages can be seen in the high degree of self-shaped reedmergnerite. Under the cathodoluminescence, reedmergnerite emits blue light with different intensities (Figure 3c). Since boron element is located at the lowest detection ability of electron probe microanalyzer (EPMA) [44], the total content of each component in reedmergnerite measured in this paper was about 79–85%, less than 100% (Table 2). The difference may be that the content of B<sub>2</sub>O<sub>5</sub> and the content of B<sub>2</sub>O<sub>5</sub> after treatment are close to the standard content of B<sub>2</sub>O<sub>5</sub> in reedmergnerite [45]. In order to enhance credibility and accuracy, the laser Raman (LR) method was used to test the reedmergnerite. The test spectra showed that the transverse coordinates of the four characteristic peaks were 230 cm<sup>-1</sup>, 600 cm<sup>-1</sup>, 1000 cm<sup>-1</sup>, and 1600 cm<sup>-1</sup>, respectively. The transverse coordinate of the main peak was 600 cm<sup>-1</sup>, which was similar to the characteristics of the Reedmergnerite Raman spectra [46] (Figure 5).

Reedmergnerite often appears with alkaline minerals. Due to the limitation of the number of drilling wells, in the samples of the Fengcheng Formation, it was found that wollastonite was mainly symbiotic with trona and shortite (Figure 4d,e). From the metasomatism relationship between them, for example, reedmergnerite starts to replace the shortite from the edge (Figure 4d), and it can be seen that the formation of reedmergnerite was later than alkaline minerals.

#### 4.3. Homogenization Temperature of Reedmergnerite Primary Fluid Inclusions

According to the phase combination and microscopic fluorescence characteristics of fluid inclusions at room temperature, the fluid inclusions of reedmergnerite can be divided into five categories: (1) liquid-only inclusions (L-O) in a single liquid phase without visible bubbles; (2) liquid-dominated two-phase inclusions (L-D) with a gas–liquid ratio less than 50%; (3) single-liquid phase oil inclusions emitting blue light under fluorescence; (4) gas–liquid two-phase oil inclusions with a gas–liquid ratio of less than 50% emitting blue light under fluorescence; (5) oil inclusions emitting yellow light under fluorescence. The occurrence of fluid inclusions mainly includes the following four types: (1) The inclusions in the growth zone (GZ) often exhibit mineral growth characteristics (Figure 6a,b), and these inclusions are considered reliable primary inclusions. Fluid inclusions within the same growth zone belong to the same associations of fluid inclusions (FIA). (2) Clustered inclusions (Figure 6c) are usually clustered in a relatively small area, and clustered inclusions may be primary or secondary. When they are primary inclusions, they belong to the same FIA. (3) Random population (RP) inclusions, which are randomly and directionally distributed in a relatively large area (Figure 6d), are of unknown origin and may be either

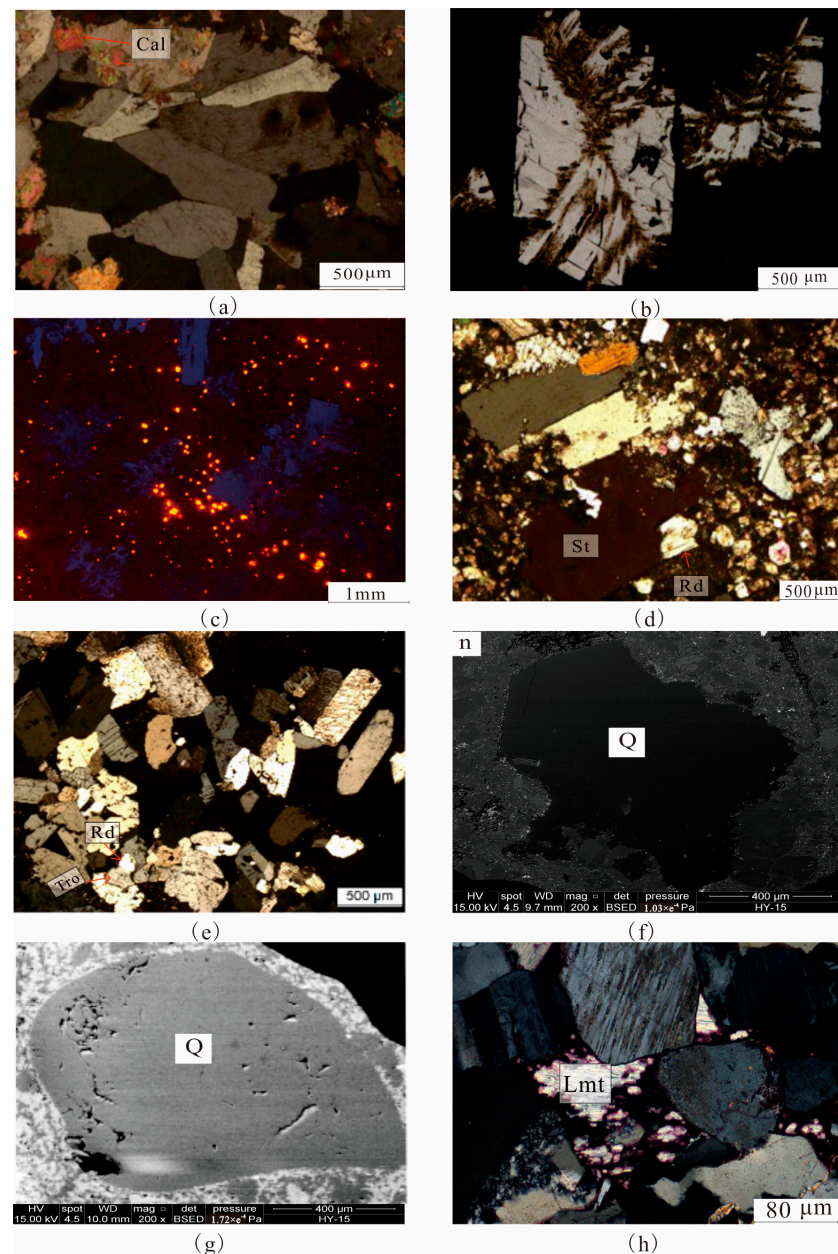
primary or secondary. In any case, such inclusions do not belong to the same FIA. (4) The inclusion in Long Trail (LT) refers to a healing crack that cuts through the mineral boundary (Figure 6e,f), the inclusion produced as a healing crack is considered a typical secondary inclusion, and the inclusion produced in the same healing crack belongs to one FIA [47].



**Figure 3.** Petrological characteristics in the Mahu Depression, Junggar Basin: (a) MY1-F2, characteristics of lamellar iron dolomite under cathodoluminescence; (b,c) FN14-F2, microscopic characteristics of massive iron dolomite and its cathodoluminescence properties; (d,e) FN14-F2, microscopic characteristics of snowflake iron dolomite and its cathodoluminescence properties; (f) FN14-F2, bright iron-poor nuclei (Cal), the number of bands indicated by 1, 2, 3, 4, 5; (g) FN14-F2, the calcite (Cal) in the belt is metasomatized almost entirely by ferric dolomite (Fer-DOL), which is metasomatized later by reedmergnerite (Rd); (h) FN14-F2, skeletal crystalline reedmergnerite with irregular radial edges.

Through systematic analysis of fluid inclusion petrography, the inclusions in the study area mainly exhibit the following five types of associations: (1) Rich liquid two-phase saline inclusions with relatively consistent gas–liquid ratios were detected in the growth zone of reedmergnerite minerals (Figure 6b). (2) A rich liquid phase two-phase brine inclusion

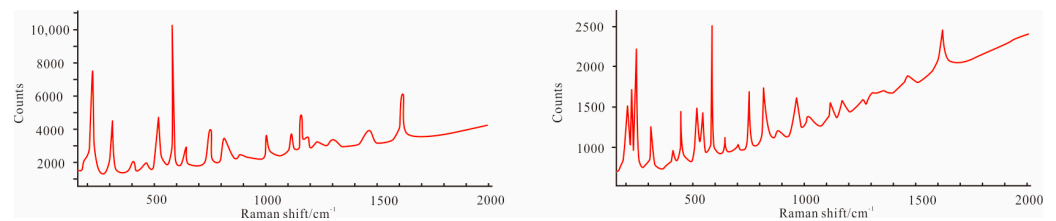
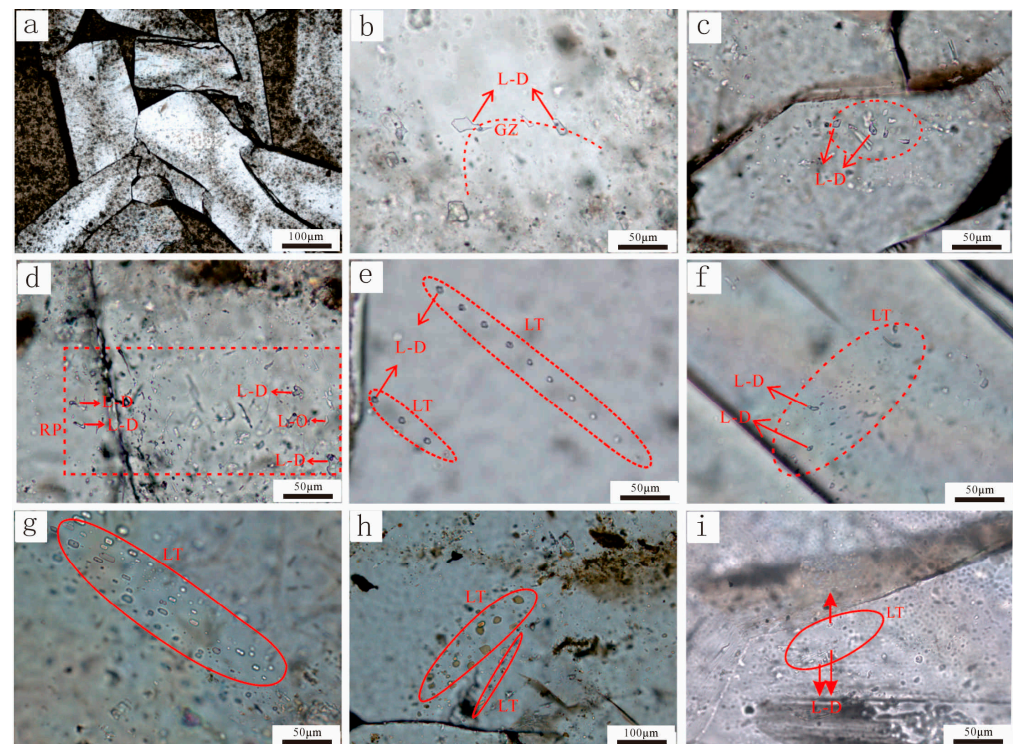
was detected in the long healing crack of cut borosilicate (Figure 6f). (3) The long healing crack of cut borosilicate was detected as a rich liquid-phase two-phase oil inclusion with green fluorescence (Figure 6g,h). (4) Rich liquid phase two-phase oil inclusions with yellow and blue fluorescence were detected in multiple long healing cracks of cut borosilicate (Figure 6i). (5) Long healing cracks in cut borosilicate were detected, with yellow fluorescent two-phase oil inclusions in the rich liquid phase and two-phase saline inclusions in the rich liquid phase.



**Figure 4.** Alkaline diagenesis characteristics in the Mahu Depression, Junggar Basin: (a) FN14-F2, wedge-shaped reedmergnerite is clustered together, and some of it contains residual calcite (Cal); (b) FN14-F2, rhomboid reedmergnerite with serrated edges; (c) FN14-F2, under cathodoluminescence, the reedmergnerite shows dark blue; (d) FN14-F2, reedmergnerite (Rd) metasomatism of shortite (St) from the edge; (e) AK1-F2, reedmergnerite (Rd) is symbiotic with trona (Tro); (f) FN14-F1, the edge of quartz grain is corroded into a serrated or bay shape; (g) MY1-F1, the internal surface of quartz was dissolved to form a “honeycomb” pit, 200 times; (h) MY1-F1, laumontite cemented between particles (Lmt).

**Table 2.** EPMA data table of reedmergnerite (wt.%).

Na <sub>2</sub> O	TiO <sub>2</sub>	SO <sub>3</sub>	SiO <sub>2</sub>	FeO	P <sub>2</sub> O <sub>5</sub>	Al <sub>2</sub> O <sub>3</sub>	MnO	K <sub>2</sub> O	MgO	BaO	CaO	B <sub>2</sub> O <sub>5</sub>	Total
10.000	-	-	70.517	-	-	-	-	0.001	0.010	0.025	-	19.447	100
10.000	-	0.010	69.767	0.028	-	-	0.043	0.012	-	-	-	20.118	99.98
13.794	-	-	71.165	0.009	0.025	0.047	-	-	0.007	-	0.005	14.948	100
11.936	0.065	-	69.377	0.017	0.017	0.068	-	0.062	0.014	0.016	0.013	18.415	100
10.012	-	0.162	69.697	0.020	0.017	0.086	-	0.088	0.027	-	-	19.891	100
10.000	0.258	-	70.632	-	-	0.094	0.009	0.008	0.028	0.007	-	18.964	100
10.063	0.080	0.031	70.288	-	-	0.010	-	0.015	-	-	-	19.513	100
10.042	-	0.005	70.015	0.004	-	0.003	0.025	0.024	-	-	0.004	19.878	100
10.072	0.032	-	64.868	0.009	0.017	0.004	0.024	0.021	0.018	-	-	20.935	96

**Figure 5.** Laser Raman spectroscopy of reedmergnerite.**Figure 6.** Fluid characteristics of the fluid inclusion in reedmergnerite. (a) FN2, reedmergnerite text. (b) FN2, Growth Zone (GZ) surrounded by fluid inclusions in reedmergnerite. (c) FN1, Cluster like distribution of fluid inclusions in reedmergnerite. (d) FN1, random distribution (RP) fluid inclusions in reedmergnerite. (e) FN3, long trail (LT) in cutting shortite crystals. (f) FN1, long trail (LT) in cutting reedmergnerite crystals. (g) FN1, long trail (LT) in cutting reedmergnerite crystals, gas liquid two-phase inclusions. (h) FN1, gas liquid two-phase inclusions. (i) FN1, long trail (LT) in cutting reedmergnerite crystals, liquid-dominated biphasic inclusions (L-D).

A total of 15 L-D fluid inclusions with relatively consistent gas–liquid ratios were detected in the growth band, forming three FIAs. The three FIAs showed consistent

temperature measurement data (Table 3), and the homogenization temperature ( $T_h$ ) range of 15 L-D fluid inclusions was 100–116 °C (Figure 7).

**Table 3.** Results of homogenization temperature of the fluid inclusion in reedmergnerite.

Borehole	Deep/m	Fluid Inclusions Occurrence	Associations of Fluid Inclusions	Type	Size/ $\mu\text{m}$	Homogenization Temperature/ $^{\circ}\text{C}$
Fengnan2	4100.58	growth zone	FIA-1	gas and liquid	20	112
				liquid	10	100
				liquid	15	111
Fengnan2	4100.58	growth zone	FIA-2	gas and liquid	5	112
				gas and liquid	4	100
				liquid	4	111
				liquid	5	112
				liquid	4	100
Fengnan2	4100.58	growth zone	FIA-3	gas and liquid	4	111
				gas and liquid	6	104
				gas and liquid	5	103
				liquid	7	109
				liquid	5	110
				liquid	7	116
				liquid	6	112

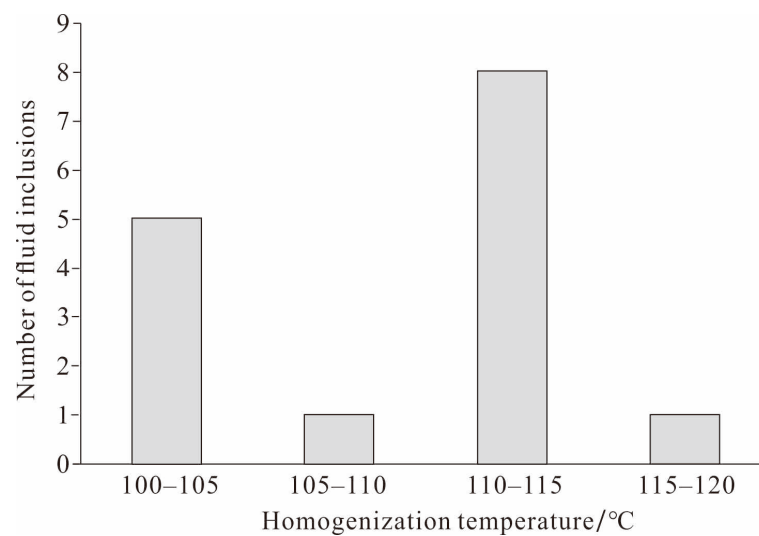


**Figure 7.** Homogenization temperature histogram of reedmergnerite primary fluid inclusions.

## 5. Discussion

### 5.1. Types of Alkaline Lake Diagenesis and Their Causes

Diagenetic minerals, such as iron dolomite and laumontite, can form under normal burial temperature conditions. However, the formation of reedmergnerite occurs at relatively high temperatures [42,43]. According to the homogenization temperature of reedmergnerite primary fluid inclusions, alkaline diagenesis of the Fengcheng Formation was divided into two stages, which are early stage ( $\leq 100$  °C) and middle stage ( $> 100$ ), with the early stage corresponding to low-temperature alkaline diagenesis and middle stage corresponding to medium-high-temperature alkaline diagenesis. The manifestations of low-temperature alkaline diagenesis include the formation of iron dolomite rings, quartz dissolution, and cementation of laumontite, and the appearance of reedmergnerite marked the medium-high-temperature alkaline diagenesis.

### 5.1.1. Indicative Significance of Iron Dolomite Ring

Because the content of  $\text{Fe}^{2+}$  is closely related to the CL luminescence intensity of the band [30,43,44], it is important to analyze the source of  $\text{Fe}^{2+}$ . There are two sources of Fe in Fengcheng Formation iron dolomite: (1) The upwelling of marine brine due to the action of capillary force brought a large amount of Fe. The residual marine brine of the Jiamuhe Formation under the Fengcheng Formation invaded [48], bringing abundant elements such as Fe, Mn, and Mg [49]. (2) Meanwhile, the various microorganisms in the Fengcheng Formation are beneficial for the enrichment of iron elements [17,24]. (3) Fe elements contributed with medium basic volcanic ash. Volcanic ashes are widely distributed in Fengcheng Formation [48], and medium basic volcanic ashes contain a large amount of Mg, Fe, and other elements [50], which release a large amount of  $\text{Fe}^{2+}$  in the process of the devitrification of volcanic glasses.

### 5.1.2. Quartz Dissolution

Quartz dissolution is a typical alkaline diagenetic phenomenon [51,52]. Three different quartz dissolution phenomena were found in the core thin sections of the Fengcheng Formation: (1) the edge of quartz particles is dissolved, and it becomes serrated or bay-shaped (Figure 4f); (2) the quartz particles are corroded inside, and microscopic dense “honeycomb” corrosion pits can be seen on the mineral surface in SEM tests (Figure 4g); (3) quartz grains develop an irregular linear distribution of fractures, and some of the fractures are locally widened by further corrosion.

The dissolution of quartz in the Fengcheng Formation was affected by  $\text{Na}^+$ , temperature, and alkalinity, and it occurred during the burial diagenetic period. Quartz dissolution is closely related to the alkaline diagenetic environment [1,17,51,53], especially with the alkaline cation  $\text{Na}^+$ , which can form sodium silicate on the surface of quartz particles through hydration reactions, and then, they crack to cause quartz erosion [54–56]. The Fengcheng Formation rocks were formed in an alkaline lake environment [39–44,56,57]. The Fengcheng Formation volcanic rocks are sodium-rich volcanic rocks, and the content of  $\text{Na}_2\text{O}$  in the volcanic rocks is much higher than that of  $\text{K}_2\text{O}$  [58]. The Na element mainly exists in albite. The albite content in the volcanic rocks of the Fengcheng Formation is high [33], and the hydrolysis of albite increases the content of  $\text{Na}^+$ , which causes the cations in the alkaline lake water to be dominated by  $\text{Na}^+$  [40]. The alkaline diagenetic environment rich in  $\text{Na}^+$  is favorable for quartz dissolution because the high  $\text{Na}^+$  content increases the probability of  $\text{Na}^+$  forming complexes on the quartz surface.

Under the same conditions, the dissolution rate of quartz at a high temperature (430 °C) is 11 orders of magnitude faster than that at a relatively low temperature (25 °C) [59], that is. High temperature is beneficial for the dissolution of quartz. In addition, the pH value also affects the dissolution of quartz. When the predecessors conducted hydrothermal experiments on the dissolution of quartz in an alkaline environment at a temperature of 130 °C and a pH value of 9.5, the quartz was significantly dissolved [52]. Therefore, the ground temperature was calculated according to the burial depth of the Fengcheng Formation, and it was concluded that such temperature conditions can be satisfied [59,60]. The pH value of the alkaline lake during the deposition of the Fengcheng Formation was in the range of 9–11 [25]. During the diagenetic stage, the alkalinity decreased, but the temperature increased. The temperature change had a greater impact on the quartz dissolution than the pH change [52]. Therefore, the Fengcheng Formation has the condition of quartz dissolution in a burial alkaline environment. In addition, due to the fact that quartz dissolution is positively correlated with  $\text{Na}^+$ , the catalytic activity of the alkaline cation  $\text{Na}^+$  increases with the increase of alkalinity [50,58], and the increase of alkalinity can promote the dissolution of quartz. Regarding temperature and alkalinity, the dissolution of quartz is intensified with the rise of temperature in the middle- and high-temperature alkaline diagenetic stage. For example, the serrate dissolution of quartz edge is intensified and then becomes harbored, and the local dissolution of internal cracks in quartz minerals is intensified and widened.

### 5.1.3. Cementation of Laumontite

The laumontite in the Fengcheng Formation rocks mostly exists in the state of sheet-like cement (Figure 3h), which is an authigenic aluminosilicate mineral with a high content of  $\text{Ca}^{2+}$  formed in a neutral-alkaline environment, and the corresponding pH value is mostly 7–10 [61]. This type of zeolite cementation is closely related to the properties of volcanic materials and their hydrolysis [62,63]. As the stratum was buried and the temperature of the stratum rose, a large number of low-temperature unstable minerals contained in the intermediate–basic volcanic rocks (substances) were hydrolyzed to form laumontite cement in an alkaline environment [64]. With the evolution of organic matter in the Fengcheng Formation, a large amount of  $\text{CO}_2$  and short-chain organic fatty acids were released [64]. The atmospheric water infiltrated along the Kebai-Wuxia fault belt, and pore water was formed by the dehydration of clay minerals [65]. Under the combined action, the early cemented laumontite was dissolutive.

### 5.1.4. Formation of Reedmergnerite

The appearance of reedmergnerite marks the middle-high temperature alkaline diagenesis of the Fengcheng Formation, and its formation is closely related to the hydrothermal fluid. The main evidence is as follows: (1) During the period of the Fengcheng Formation, different rare earth element distribution models showed that the fluids mainly came from endogenous fluids in different parts, including subduction zones, crustal, and mantle sources, and the boron required for reedmergnerite mainly came from deep alkaline hydrothermal fluids [56,66]. (2) The measurement of boron isotope  $\delta^{11}\text{B}$  showed that the fluids of different forms of reedmergnerite in the Fengcheng Formation were from the same source, and the fluid may come from deep hydrothermal sources [56]. (3) Reedmergnerite is widely developed near the fault, and during the Fengcheng Formation, regarding the volcanic activity [67], boron-rich hydrothermal fluids affected by volcanic activity could migrate along developed fault networks. (4) Reedmergnerite was formed in a closed alkaline lake environment [41], and it was not easy for enthetic materials to enter the lake basin through relatively normal and gentle migration. The hydrothermal fluid in the deep is more capable of entering this closed environment under the external force of the huge energy [56], bringing the required substances. (5) The hydrothermal fluid can provide a sufficient reaction temperature, which can reach the experimental temperature required for the synthesis of reedmergnerite [46,47], while the reedmergnerite in the Fengcheng Formation was developed in the Feng 2, with a burial depth greater than 3000 m [56], and in 2018, Rao Song studied the thermal history recovery characteristics of the Junggar Basin by using paleo-temperature scale methods, such as vitrinite reflectance and fission track [60], and found that the geothermal gradient of the Fengcheng Formation was 5–3 °C/100 m. The formation temperature of the reedmergnerite development layer was about 140 °C (the average geothermal gradient is 4 °C, and the annual average temperature is about 20 °C), which cannot reach the temperature threshold required for the formation of reedmergnerite, while the hydrothermal fluid becomes capable of providing the greatest possible chance of such a high temperature.

According to the phenomenon actually observed in the thin slices, it was found that reedmergnerite had a metasomatism relationship with alkaline minerals, such as sodium-calcium carbonate (Figure 4f), trona (Figure 4g), and carbonate minerals (Figures 3h and 4a,b). Alkaline minerals and carbonate minerals have certain commonalities. Regarding chemical composition, alkaline minerals are carbonate minerals with different  $\text{Na}^+$  contents. Because the composition of carbonate minerals and alkaline minerals is different from that of reedmergnerite, two processes of dissolution and recrystallization were involved in the metasomatism [57]. Different dissolution degrees, different crystal habits, and different order degrees during recrystallization may be important reasons for the formation of different forms of reedmergnerite [49].

At present, there are different opinions on the division of the formation period of reedmergnerite, including the buried diagenetic period and quasi-contemporaneous

period [24,39,46,56,63]. Temperature and pressure are the key factors in the formation of reedmergnerite [63]. The burial was shallow in the quasi-contemporaneous period. The temperature and pressure were not up to the formation conditions of reedmergnerite, and the carbonate minerals and alkaline minerals metasomatized by reedmergnerite were mainly developed in the Feng 2 Member, with a burial depth greater than 3000 m [56]. Therefore, it was speculated that the reedmergnerite was mainly formed by the metasomatism of carbonate minerals and alkaline minerals formed earlier under the action of an abnormal hydrothermal factor during burial diagenesis.

### 5.2. Diagenetic Evolutionary Sequence of Fengcheng Formation Shale Series in Mahu Sag

Characterized by the vitrinite reflectance (Ro) of mudstone in the Fengcheng Formation and supported by inclusion temperature, most reservoirs in the Fengcheng Formation are in middle diagenetic stage A, and a small part of them enter middle diagenetic stage B [68,69].

#### 5.2.1. Devitrification and Hydrolysis

Volcanic glass material is unstable and often altered or devitrified to form stable clay minerals and zeolite under the action of volcanic activities and tectonic movements. The Fengcheng Formation contains a large amount of volcanic vitreous originally, which is widely distributed in clastic rock debris and volcanic rock matrix. Influenced by the environment, it can release a large amount of  $K^+$ ,  $Na^+$ ,  $Ca^{2+}$ ,  $Mg^{2+}$ , and saline and alkaline interlayer pore water.

#### 5.2.2. Diagenetic Mineral Precipitation Sequence

The first mineral to emerge from the solution was montmorillonite [70]. In the Fengcheng Formation, this part of montmorillonite was gradually transformed to form the Aemon mixed layer. With the further reaction, the salinity and alkalinity of the interlayer solution rose to the range of feldspar precipitation, and the feldspar precipitated was associated with clay minerals, followed by zeolite and quartz precipitation. The early zeolite was unstable, and with a further increase in temperature, it further generated zeolite and feldspar and released calcium ions, and the surplus calcium ions promoted the formation of calcite [61,71]. Under the conditions of temperature and pressure, and the abundant magnesium and iron ions in the solution, part of the montmorillonite was transformed into chlorite. Along with the hydrolytic alteration of volcanic glass materials, magnesite minerals, such as pyroxene, hornblende, biotite, and feldspar phenocrysts, crystal chips, and potassium feldspar in pyroclastic materials also have some chlorite (Figure 8). At the same time, the authigenic minerals precipitated under such environmental conditions are as follows: (1) bicarbonate minerals (carbonaceous calcium stone, trona, carbonaceous sodium magnesite, etc.); (2) salt minerals (sodium silicate, salt, etc.); (3) aluminum silicate minerals (potassium feldspar, albite, zeolite, etc.); (4) calcium and magnesium carbonate minerals (dolomite, calcite, etc.); (5) siliceous minerals (quartz, opal, etc.) [72].

The alteration process of the Fengcheng Formation can be classified as follows: (1) hydrolysis of volcanic glass, generation of montmorillonite, generation of zeolite minerals and related transformation, albitization; (2) chlorite influenced by magnesium and iron ions; (3) feldspar alteration, formation of chlorite and calcite, rest albite. In particular, hydrolysis occurred in the early diagenetic A stage. Dolomite formation can be divided into three stages, most of which were in early diagenetic stage B. Salt minerals were formed in the same generation. There are three phases of dissolution, which are scattered from the late early diagenetic stage to the middle diagenetic stage B (Figure 8).

### 5.3. Alkaline Sedimentary Evolution and Diagenetic Model of Fengcheng Formation Shale Series in Mahu Sag

Based on core slices from wells FN1, FN14, AK-1, and MH7 in the Mahu sag, combined with the literature data, the sedimentary evolution and the diagenetic model of the Fengcheng Formation in the alkaline lake environment were established from the aspects

of climate, provenance, diagenetic environment, and underground fluids (Figure 9), which can be roughly divided into four stages: before the deposition of the Fengcheng Formation, during the deposition of the Fengcheng Formation, the low-temperature alkaline burial diagenetic stage, and the hydrothermal-related medium-high-temperature alkaline diagenetic stage.

Diagenesis		Syngenetic period	Early diagenesis A stage	Early diagenesis B stage	Middle diagenesis A stage	Middle diagenesis B stage	
Hydrolysis reaction			=====	=====			
Devitrification action			=====				
Major diagenetic minerals precipitate	Carbonate	Dolomite	=====	=====			
		Calcite	=====	=====			
	Alumino-silicate	Montmorillonite		=====			
		Feldspar				=====	=====
		Zeolite				=====	=====
	Sulfate	Anhydrite			=====		
		Other salt minerals	Shortite		=====		
	Reedmergerite					=====	
	Hydrocarbon sodalite		=====				
	Chlorocarbonite		=====				
	Sodalite		=====				
	Halite		=====				
	Siliceous minerals	Trona	=====				
		Quartz			=====	=====	=====
Aluminosilicate dissolution				=====	=====	=====	
Saline minerals dissolution				=====	=====	=====	
Siliceous minerals dissolution			=====	=====			

Figure 8. Sequence diagram of the diagenetic evolution of the Fengcheng Formation in Mahu sag.

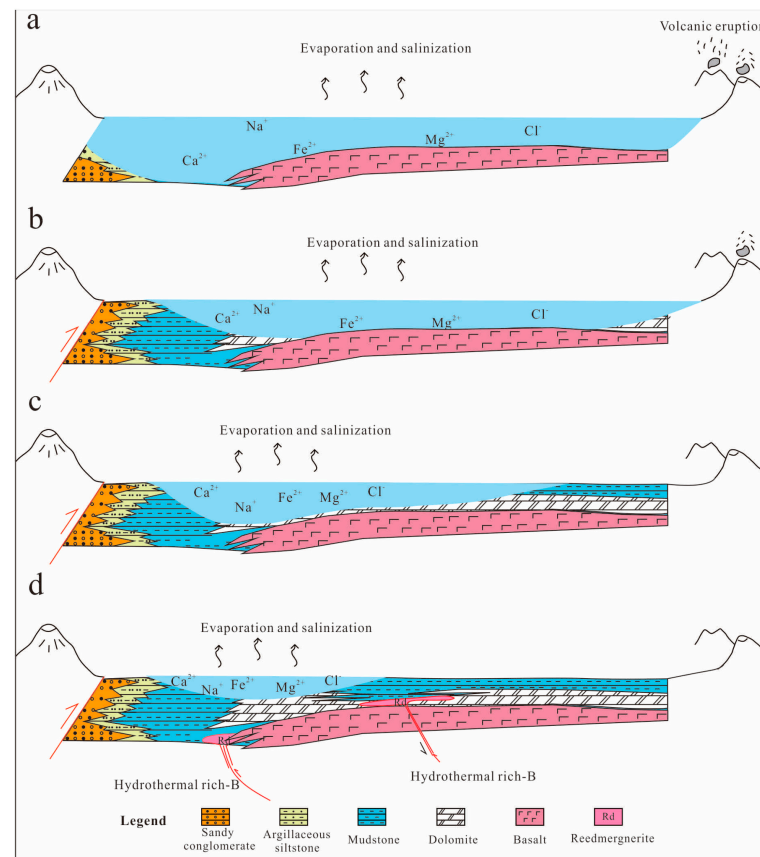


Figure 9. Alkaline sedimentary evolution–diagenesis model of the Fengcheng Formation (the faults shown are schematic faults [24,39]). (a) before the deposition of the Fengcheng Formation (b) during the sedimentation of the Fengcheng Formation. (c) low-temperature alkaline burial diagenesis. (d) medium-high-temperature alkaline diagenesis.

Before the deposition of the Fengcheng Formation, in the arid/semi-arid climate, the lake water was evaporated and concentrated [41], resulting in a gradual increase in the alkalinity of the water body [57,62,63]. In addition, due to active volcanic activity, a large number of volcanic rocks developed at the bottom of the lake basin, and the low-temperature unstable minerals contained in the volcanic rocks were hydrolyzed, which provided  $\text{Na}^+$ ,  $\text{Ca}^{2+}$ ,  $\text{Mg}^{2+}$ , and  $\text{Fe}^{2+}$  for the water body, which laid the material foundation for diagenesis and alkaline lake formation (Figure 9a).

During the deposition of the Fengcheng Formation, there were  $\text{Cl}^-$ ,  $\text{CO}_3^{2-}$ ,  $\text{SO}_4^{2-}$ , and other anions in the lake basin. During the process of lake basin shrinkage and alkalization, the concentration of ions gradually increased, collided, and combined with each other, and a large number of Mg-Ca carbonate minerals and alkaline minerals with anions of  $\text{CO}_3^{2-}$  appeared. In the presence of  $\text{Mg}^{2+}$ ,  $\text{Na}^+$ , and  $\text{Ca}^{2+}$  plasmas, the order of binding with  $\text{HCO}_3^-$  and  $\text{CO}_3^{2-}$  is  $\text{Ca}^{2+}$ ,  $\text{Mg}^{2+}$ , and  $\text{Na}^+$  [73], with  $\text{CaCO}_3$  precipitation before  $\text{MgCO}_3$ . After calcite precipitation, the lake water was stratified under the action of evaporation and concentration, which promoted the development of argillaceous sediments rich in organic matter [28]. The different types of organic matter were mainly from that organic matter [74,75], and their decay products were conducive to the large-scale development of carbonate minerals, forming lamellar carbonate mineral layers (mainly calcite) and argillaceous sediment layers. At this time, due to the large consumption of  $\text{Ca}^{2+}$ , the  $\text{Mg}^{2+}/\text{Ca}^{2+}$  ratio in the water body increased, and the  $\text{Fe}^{2+}$  was contributed by the volcanic tuff material. The microcrystal dolomite was also deposited [76]. The extensive development of carbonate minerals consumed a large amount of  $\text{Ca}^{2+}$  and  $\text{Mg}^{2+}$ , while the content of  $\text{Na}^+$  increased relatively, and the consumed  $\text{CO}_3^{2-}$  was continuously supplemented by volcanic activity.

With the further shrinkage of the lake basin water body, alkalinity reached the maximum amount,  $\text{Na}^+$  and  $\text{CO}_3^{2-}$  tended to be saturated, and  $\text{Na}^+$  containing alkaline minerals such as trona and sodium-calcium carbonate was formed successively. Finally, the climate became hot and humid, and the water level rose. Under the supply of terrigenous detrital materials, materials such as mud and sand were deposited, and the sedimentary strata of the Fengcheng Formation were deposited (Figure 9b).

In the low-temperature alkaline diagenetic stage, the residual marine brine in the Carboniferous and Jiamuhe Formations underlying the Fengcheng Formation from the mid-Permian to the mid-Jurassic period [67], entering into the pores and fractures of the Fengcheng Formation along the fault under tectonic compression, it brought abundant elements such as Fe, Mn, and Mg [73] and cemented around the early calcite or calcite with a low degree of dolomitization, and the local distribution of fine-grained iron dolomite with clear ring was formed. With the surging of residual marine brine,  $\text{Na}^+$  was also present. In addition, the two necessary conditions of alkaline formation water and the rising temperature due to the formation's burial were also present. The dissolution of quartz occurred, and the "salt effect" of  $\text{Mg}^{2+}$ ,  $\text{K}^+$ , and  $\text{Ca}^{2+}$  in formation water further promoted the dissolution of quartz [52]. In this stage, in addition to the formation of iron dolomite and quartz dissolution, the cementation of laumontite also occurred under the background of alkaline diagenesis, low temperature, and the supply of  $\text{Mg}^{2+}$  and  $\text{Fe}^{2+}$  (Figure 9c).

The hydrocarbon source rocks of the Fengcheng Formation did not enter the oil generation threshold until the end of the Permian period [77], and kerogen began to transform into oil and gas. This process was accompanied by the formation of oxalic acid and acetic acid [13], where local pore fluid pH dropped and became acidic, resulting in the dissolution of early turbidite, iron dolomite, and alkaline minerals. The acidic fluid generated by oil and gas was neutralized by alkaline formation water and alkaline minerals, and the whole presented an alkaline diagenetic environment. During the middle-high-temperature alkaline diagenesis stage, the hydrothermal activity was intense at the end of the Triassic period [64], and the B-rich hydrothermal fluid migrated and upwelled along the fault. Reedmergnerite was formed by alkaline minerals containing  $\text{Na}^+$ . Correspondingly, the mineral assemblages of reedmergnerite + calcite + iron dolomite, reedmergnerite + shortite, and

reedmergnerite + mineral assemblages of trona can be found in the parts with incomplete metasomatism. Under the influence of the intercalated horizon of the fault, the distribution and morphology of the metasomatic minerals, and other factors, banded and agglomerated reedmergnerite was formed. As the overlying material continued to deposit, the burial depth increased. When the stone was enriched to a certain extent, it formed reedmergnerite-rich rocks (Figure 9d). Marked by the appearance of reedmergnerite, medium-high-temperature alkaline diagenesis occurred in the center and slope of the Mahu sag and near the fault zone, connecting the deep fluid and alkaline mineral layer and the carbonate layer [56].

## 6. Conclusions

In this paper, the types of shale series developed in the Fengcheng Formation in the Mahu sag include carbonate rocks, terrigenous detrital rocks, and alkaline mesobasic volcanic rocks, and there are bands and agglomerates rich in reedmergnerite. Under the combined influence of the supply of sodium-rich sources, an alkaline lake characterized by the development of alkaline minerals was formed, and experienced alkaline deposition and diagenesis was formed in an alkaline environment.

There were three types of diagenetic mineral assemblages and two types of alkaline diagenesis developed in the shale series of the Fengcheng Formation. The three mineral combinations include: carbonate mineral combination (calcite + iron dolomite), reedmergnerite and carbonate mineral combination (reedmergnerite + calcite + iron dolomite), and reedmergnerite and alkaline minerals combination (reedmergnerite + shortite + trona). According to the diagenetic temperature, the alkaline diagenesis of the Fengcheng Formation can be divided into two types: low-temperature alkaline burial diagenesis and medium-high-temperature alkaline diagenesis. The former is characterized by the formation of iron dolomite rings, quartz dissolution, and laumontite cementation, while the latter is characterized by the abundant presence of reedmergnerite.

Under the promotion of a long-term arid/semi-arid climate, based on underground fluids (hydrothermal and brine) and alkaline medium-basic volcanic parent rocks (substances) as the main material sources, in the special alkaline diagenetic environment of alkali lake, the alkaline sedimentary evolution–diagenetic model of the Fengcheng Formation, which was affected by climate, provenance, diagenetic environment, and underground fluid, was established. The model was divided into four stages: before the deposition of the Fengcheng Formation, sedimentary, low-temperature alkaline burial diagenesis, and hydrothermally related medium-high-temperature alkaline diagenesis.

**Author Contributions:** Conceptualization, methodology, and writing, B.B., J.L. and C.D.; review and editing, W.H. and C.D.; validation, Y.B. and X.C.; analysis and investigation, M.Z. and H.L.; supervision and editing, H.Z. All authors have read and agreed to the published version of the manuscript.

**Funding:** National Natural Science Foundation of China (No. 42090025, 42072186), Petrochina Co., Ltd. Technology Support Program (2022DQ0525, 2021–DJ2203).

**Institutional Review Board Statement:** Not applicable.

**Informed Consent Statement:** Not applicable.

**Data Availability Statement:** Data are contained within the article.

**Acknowledgments:** The authors express their gratitude to Zhenkun Yu for support and assistance during the field visit and data collection.

**Conflicts of Interest:** Authors Bin Bai, Wenjun He and Ying Bai were employed by the company PetroChina. The remaining authors declare that the research was conducted in the absence of any commercial or financial relationships that could be construed as a potential conflict of interest. The authors declare that this study received funding from Petrochina Co., Ltd. The funder was not involved in the study design, collection, analysis, interpretation of data, the writing of this article or the decision to submit it for publication.

## Abbreviations

The following abbreviations are used in this manuscript:

EPMA	electron probe microanalysis
SEM	scanning electron microscope
CL	cathode luminescence
LR	laser Raman
Cal	calcite
Fer-DOL	ferric dolomite
Rd	reedmergnerite
Tro	Trone
St	shortite
Lmt	laumontite cemented between particles

## References

1. Kuang, L.C.; Tang, Y.; Lei, D.W.; Chang, Q.S.; Ouyang, M.; Hou, L.H.; Liu, D.G. Formation conditions and exploration potential of tight oil in the Permian saline lacustrine dolomitic rock, Junggar Basin, NW China. *Pet. Explor. Dev.* **2012**, *39*, 657–667. [\[CrossRef\]](#)
2. Kuang, L.C.; Cui, X.K.; Zou, C.N.; Hou, L.H. Oil accumulation and concentration regularity of volcanic lithostratigraphic oil reservoir: A case from upper-plate Carboniferous of KA-BAI fracture zone, Junggar Basin. *Pet. Explor. Dev.* **2007**, *34*, 285–290.
3. Yu, K.; Cao, Y.; Qiu, L.; Sun, P. The hydrocarbon generation potential and migration in an alkaline evaporate basin: The Early Permian Fengcheng Formation in the Junggar Basin, northwestern China. *Mar. Pet. Geol.* **2018**, *98*, 12–32. [\[CrossRef\]](#)
4. Jagniecki, E.A.; Jenkins, D.M.; Lowenstein, T.K.; Carroll, A.R. Experimental Study of Shortite (Na<sub>2</sub>Ca<sub>2</sub>(CO<sub>3</sub>)<sub>3</sub>) Formation and Application to the Burial History of the Wilkins Peak Member, Green River Basin, Wyoming, USA. *Geochim. Cosmochim. Acta* **2013**, *115*, 31–45. [\[CrossRef\]](#)
5. Smith, M.E.; Carroll, A.R.; Singe, B.S. Synoptic Reconstruction of a Major Ancient Lake System: Eocene Green River Formation, Western United States. *Geol. Soc. Am. Bull.* **2008**, *120*, 54–84. [\[CrossRef\]](#)
6. Javier, G.V.; Ibrahim, G.; Cahit, H.; Eva, P. Genetic Model for Na-Carbonate Mineral Precipitation in the Miocene Beypazarı Trona Deposit, Ankara Province, Turkey. *Sediment. Geol.* **2013**, *294*, 315–327.
7. Meng, T.; Liu, P.; Qiu, L.W.; Wang, Y.S.; Liu, Y.L.; Lin, H.M.; Cheng, F.Q.; Qu, C.S. Formation and distribution of the high quality reservoirs in a deep saline lacustrine basin: A case study from the upper part of the 4th member of Paleogene Shahejie Formation in Bonan sag, Jiyang depression, Bohai Bay Basin, East China. *Pet. Explor. Dev.* **2017**, *44*, 896–906. [\[CrossRef\]](#)
8. Tang, Y.; Lyu, Z.X.; He, W.J.; Qing, Y.H.; Li, X.; Song, X.Z.; Yang, S.; Cao, Q.M.; Qian, Y.X.; Zhao, X.M. Origin of dolomites in the Permian dolomitic reservoirs of Fengcheng Formation in Mahu Sag, Junggar Basin, NW China. *Pet. Explor. Dev.* **2023**, *50*, 38–50. [\[CrossRef\]](#)
9. Jiang, F.J.; Hu, M.L.; Hu, T.; Lyu, J.H.; Huang, L.L.; Liu, C.L.; Jiang, Z.X.; Huang, R.D.; Zhang, C.X.; Wu, G.Y.; et al. Controlling factors and models of shale oil enrichment in Lower Permian Fengcheng Formation, Mahu Sag, Junggar Basin, NW China. *Pet. Explor. Dev.* **2023**, *50*, 706–718. [\[CrossRef\]](#)
10. Tang, Y.; Cao, J.; He, W.J.; Guo, X.G.; Zhao, K.B.; Li, W.W. Discovery of shale oil in alkaline lacustrine basins: The Late Paleozoic Fengcheng Formation, Mahu Sag, Junggar Basin, China. *Pet. Sci.* **2021**, *18*, 1281–1293. [\[CrossRef\]](#)
11. Qiu, L.W.; Jang, Z.X.; Cao, Y.C.; Qiu, R.H.; CHEN, W.X.; TU, Y.F. Alkaline diagenesis and its influence on a reservoir in the Biyang depression. *Sci. China Ser. D* **2002**, *45*, 643–653. [\[CrossRef\]](#)
12. Li, S.Y.; Tian, J.C.; Lin, X.B.; Zuo, Y.H.; Kang, H.; Yang, D.D. Effect of alkaline diagenesis on sandstone reservoir quality: Insights from the Lower Cretaceous Erlan Basin, China. *Energy Explor. Exploit.* **2002**, *38*, 434–453. [\[CrossRef\]](#)
13. Zhang, S.B.; Liu, Z.; Liu, H.J.; Song, Y.H.; Li, X.M.; Xu, T. Alkali Diagenesis of Xujiache Sandstone in Hebaochang Block in Sichuan Basin. *Xingjiang Pet. Geol.* **2011**, *32*, 464–468.
14. Cao, T.Y.; Zhong, D.K.; Niu, S.L.; Sun, H.T.; Cao, X.; Wang, F. Alkaline Diagenesis and Porosity Evolution of Zhu hai Formation Reservoirs in Eastern Huizhou Sag. *Acta Sedimentol. Sin.* **2020**, *38*, 1327–1337.
15. Zhu, H.H.; Zhong, D.K.; Yao, J.L.; Sun, H.T.; Niu, X.B.; Liang, X.W.; You, Y.; Li, X. Alkaline diagenesis and its effects on reservoir porosity: A case study of Upper Triassic Chang 7 Member tight sandstone in Ordos Basin, NW China. *Pet. Explor. Dev.* **2015**, *42*, 56–65. [\[CrossRef\]](#)
16. Hu, T.; Pang, X.Q.; Jiang, S.; Wang, Q.F.; Xu, T.W.; Lu, K.; Huang, C.; Chen, Y.Y.; Zheng, X.W. Impact of Paleosalinity, Dilution, Redox, and Paleoproductivity on Organic Matter Enrichment in a Saline Lacustrine Rift Basin: A Case Study of Paleogene Organic-Rich Shale in Dongpu Depression, Bohai Bay Basin, Eastern China. *Energy Fuels* **2008**, *32*, 5045–5061. [\[CrossRef\]](#)
17. Chen, Z.Y.; Chen, J.F.; Zhong, N.N.; Fei, W.W.; Dong, Q.W.; Chen, J.; Wang, Y.Y. The geneses of sedimentary organic matter with anomalous <sup>13</sup>C-enriched isotopic composition in saline and freshwater lakes: A case study of lacustrine source rocks from Dongpu and Qikou sags, Bohai Bay Basin, eastern China. *Mar. Pet. Geol.* **2020**, *118*, 104434. [\[CrossRef\]](#)
18. Wang, K.; Pang, X.Q.; Zhang, H.G.; Zhao, Z.F.; Su, S.C.; Hui, S.S. Characteristics and genetic types of natural gas in the northern Dongpu Depression, Bohai Bay Basin, China. *J. Pet. Sci. Eng.* **2018**, *170*, 453–466. [\[CrossRef\]](#)

19. Tan, X.F.; Tian, J.C.; Li, Z.B.; Zhang, S.P.; Wang, W.Q. Diagenesis evolution of fragmental reservoir in alkali sediment environment-taking the Member 4 of Shahejie Formation of steep-slope zone in Dongying sag, Shandong, China for example. *Geol. Bull. China* **2010**, *4*, 535–543.
20. Tang, W.B.; Zhang, Y.Y.; Georgia, P.P.; David, J.W.P.; Guo, Z.J.; Li, W. Permian to early Triassic tectono-sedimentary evolution of the Mahu sag, Junggar Basin, western China: Sedimentological implications of the transition from rifting to tectonic inversion. *Mar. Pet. Geol.* **2021**, *123*, 104730. [[CrossRef](#)]
21. He, D.F.; Li, D.; Fan, C.; Yang, X.F. Geochronology, geochemistry and tectonostratigraphy of Carboniferous strata of the deepest Well Moshen-1 in the Junggar Basin, northwest China: Insights into the continental growth of Central Asia. *Gondwana Res.* **2013**, *24*, 560–577. [[CrossRef](#)]
22. Cao, J.; Lei, D.; Li, Y.; Tang, Y.; Chang, Q.; Abulimit, I.; Wang, T. Ancient high-quality alkaline lacustrine source rocks discovered in the Lower Permian Fengcheng Formation, Junggar Basin. *Acta Pet. Sin.* **2015**, *36*, 781–790. [[CrossRef](#)]
23. Cao, J.; Xia, L.W.; Wang, T.T.; Zhi, D.M. An alkaline lake in the Late Paleozoic Ice Age (LPIA): A review and new insights into paleoenvironment and petroleum geology. *Earth-Sci. Rev.* **2020**, *202*, 103091. [[CrossRef](#)]
24. Zhang, Z.J.; Yuan, X.J.; Wang, M.S.; Zhou, C.M.; Tang, Y.; Chen, X.Y.; Lin, M.J.; Cheng, D.W. Alkaline-lacustrine deposition and paleoenvironmental evolution in permian fengcheng formation at the mahu sag, junggar basin, nw china. *Pet. Explor. Dev.* **2018**, *45*, 1036–1049. [[CrossRef](#)]
25. Yu, K.H.; Cao, Y.C.; Qiu, L.W.; Sun, P.P.; Jia, X.Y.; Wan, M. Geochemical characteristics and origin of sodium carbonates in a closed alkaline basin: The Lower Permian Fengcheng Formation in the Mahu Sag, northwestern Junggar Basin, China. *Palaeogeogr. Palaeoclimatol. Palaeoecol.* **2018**, *511*, 506–531. [[CrossRef](#)]
26. He, D.F.; Yin, C.; Du, S.K.; Shi, X.; Ma, H.S. Characteristics of structural segmentation of foreland thrust belts -A case study of the fault belts in the northwestern margin of Junggar Basin. *Earth Sci. Front.* **2004**, *3*, 91–101.
27. Li, D.; He, D.F.; Santosh, M.; Ma, D.L.; Tang, J.Y. Tectonic framework of the northern Junggar Basin part I: The eastern Luliang Uplift and its link with the East Junggar terrane. *Gondwana Res.* **2015**, *27*, 1089–1109. [[CrossRef](#)]
28. Cao, J.; Yao, S.P.; Jin, Z.J.; Hu, W.X.; Zhang, Y.J.; Wang, X.L.; Zhang, Y.Q.; Tang, Y. Petroleum migration and mixing in the northwestern Junggar Basin (NW China): Constraints from oil-bearing fluid inclusion analyses. *Org. Geochem.* **2006**, *37*, 827–846. [[CrossRef](#)]
29. Xu, Z.H.; Hu, S.Y.; Wang, L.; Zhao, W.Z.; Cao, Z.L.; Wang, R.J.; Shi, S.Y.; Jiang, L. Seismic sedimentologic study of facies and reservoir in middle Triassic Karamay Formation of the Mahu Sag, Junggar Basin, China. *Mar. Pet. Geol.* **2019**, *107*, 222–236. [[CrossRef](#)]
30. Chen, Z.L.; Liu, G.D.; Wang, X.L.; Gao, G.; Xiang, B.L.; Ren, J.L.; Ma, W.Y.; Zhang, Q. Origin and mixing of crude oils in Triassic reservoirs of Mahu slope area in Junggar Basin, NW China: Implication for control on oil distribution in basin having multiple source rocks. *Mar. Pet. Geol.* **2016**, *78*, 373–389. [[CrossRef](#)]
31. Liang, Y.Y.; Zhang, Y.Y.; Chen, S.; Guo, Z.J.; Tang, W.B. Controls of a strike-slip fault system on the tectonic inversion of the Mahu depression at the northwestern margin of the Junggar Basin, NW China. *J. Asian Earth Sci.* **2020**, *198*, 104229. [[CrossRef](#)]
32. Lei, D.; Chen, G.; Liu, H.; Li, X.; Abulimit, T.K.; Cao, J. Study on the forming conditions and exploration fields of the Mahu Giant Oil (Gas) Province, Junggar Basin. *Acta Geol. Sin.* **2017**, *91*, 1604–1619.
33. Zhang, G.Y.; Wang, Z.Z.; Guo, X.G.; Sun, Y.Y.; Sun, L.; Pan, L. Characteristics of lacustrine dolomitic rock reservoir and accumulation of tight oil in the Permian Fengcheng Formation, the western slope of the Mahu Sag, Junggar Basin, NW China. *J. Asian Earth Sci.* **2019**, *178*, 64–80. [[CrossRef](#)]
34. Chen, Y.B.; Cheng, X.G.; Zhang, H.; Li, C.Y.; Ma, Y.P.; Wang, G.D. Fault characteristics and control on hydrocarbon accumulation of middle-shallow layers in the slope zone of Mahu sag, Junggar Basin, NW China. *Pet. Explor. Dev.* **2018**, *6*, 1050–1060. [[CrossRef](#)]
35. Feng, C.; Li, T.; He, W.J.; Zheng, M.L. Organic geochemical traits and paleo-depositional conditions of source rocks from the Carboniferous to Permian sediments of the northern Mahu Sag, Junggar Basin, China. *J. Pet. Sci. Eng.* **2020**, *191*, 107117. [[CrossRef](#)]
36. Li, J.; Tang, Y.; Wu, T.; Zhao, J.Z.; Wu, H.Y.; Wu, W.T.; Bai, Y.B. Overpressure origin and its effects on petroleum accumulation in the conglomerate oil province in Mahu Sag, Junggar Basin, NW China. *Pet. Explor. Dev.* **2020**, *47*, 726–739. [[CrossRef](#)]
37. Yang, M.Z.; Wang, F.Z.; Zheng, J.P. Geochemistry and tectonic setting of basic volcanic rocks in Ke-Xia region, northwestern Junggar Basin. *Acta Petrol. Miner.* **2006**, *20*, 165–174.
38. Wu, W.; Li, Q.; Pei, J.X.; Ning, S.Y.; Tong, L.Q.; Liu, W.Q.; Feng, Z.D. Seismic sedimentology, facies analyses, and high-quality reservoir predictions in fan deltas: A case study of the Triassic Baikouquan Formation on the western slope of the Mahu Sag in China's Junggar Basin. *Mar. Pet. Geol.* **2020**, *120*, 104546. [[CrossRef](#)]
39. Wang, M.S.; Zhang, Z.J.; Zhou, C.M.; Yuan, X.J.; Lin, M.J.; Liu, Y.H.; Cheng, D.W. Lithological characteristics and origin of alkaline lacustrine of the Lower Permian Fengcheng Formation in Mahu Sag, Junggar Basin. *J. Paleogeogr.* **2018**, *20*, 147–162.
40. Xu, L.; Chang, Q.S.; Feng, L.L.; Zhang, N.; Liu, H. The reservoir characteristics and control factors of shale oil in Permian Fengcheng Formation of Mahu sag, Junggar Basin. *China Pet. Explor.* **2019**, *24*, 649–660.
41. Yu, K.H.; Cao, Y.C.; Qiu, L.W.; Sun, P.; Yang, Y.Q.; Qu, C.S.; Wan, M. Characteristics of alkaline layer cycles and origin of the Lower Permian Fengcheng Formation in Mahu sag, Junggar Basin. *J. Paleogeogr.* **2016**, *18*, 1012–1029.
42. You, X.L.; Jia, W.Q.; Xu, F.; Liu, Y. Mineralogical characteristics of ankerite and mechanisms of primary and secondary origins. *Earth Sci.* **2018**, *43*, 4046–4055.

43. Pagel, M.; Barbin, V.; Blanc, P.; Ohnenstetter, D. *Application of Cathodoluminescence to Carbonate Diagenesis*, 1st ed.; Springer: Berlin, Germany, 2000; pp. 271–301.
44. Axel, G.; Detlev, K.R.; Jan, M.; Rolf, D.N.; Andreas, S. Quantitative high resolution cathodoluminescence spectroscopy of diagenetic and hydrothermal dolomites. *Sediment. Geol.* **2001**, *140*, 191–199.
45. Braith, J.R. Cathodoluminescence in Quaternary carbonate deposits. *Sediment. Geol.* **2016**, *337*, 29–35. [[CrossRef](#)]
46. Goldstein, H.R. Systematics of fluid inclusions in diagenetic minerals. *SEPM Short Course* **1994**, *31*, 199.
47. Eugster, H.P.; Mciver, N.L. Boron analogues of alkali feldspars and related silicates. *Bull. Geol. Soc. Am.* **1959**, *70*, 1598.
48. Hou, L.H.; Zou, C.N.; Liu, L.; Wen, B.H.; Wu, X.Z.; Wei, Y.Z.; Mao, Z.G. Geologic essential elements for hydrocarbon accumulation with in Carboniferous volcanic weathered crusts in Xinjiang, China. *Acta Pet. Sin.* **2012**, *33*, 533–540.
49. Xue, J.J.; Sun, J.; Zhu, X.M.; Liu, W.; Zhu, S.F. Characteristics and Formation Mechanism for Dolomite Reservoir of Permian Fengcheng Formation in Junggar Basin. *Geoscience* **2012**, *26*, 755–761.
50. Qiu, L.W.; Jiang, Z.X.; Chen, W.X. A new type of secondary porosity--quartz dissolution porosity. *Acta Sedimentol. Sin.* **2002**, *4*, 621–627.
51. Qu, X.Y.; Chen, X.; Qiu, L.W.; Zhang, M.L.; Zhang, X.J. Genesis of secondary pore of quartz dissolution type and its influences on reservoir: Taking the tight sandstone reservoir in the Upper Paleozoic of Daniudi gas field as an example. *Oil Gas Geol.* **2015**, *36*, 804–813.
52. Liu, J.K.; Peng, J.; Shi, Y.; Bao, Z.F.; Sun, Y.L.; Liu, X.M.; Zhang, Z. The genesis of quartz dissolution in tight sand reservoirs and its impact on pore development: A case study of Xujiache Formation in the transitional zone of Central-Southern Basin. *Acta Pet. Sin.* **2015**, *36*, 1090–1097.
53. Rimstidt, J.D.; Zhang, Y.L.; Zhu, C. Rate equations for sodium catalyzed amorphous silica dissolution. *Geochim. Cosmochim. Acta* **2016**, *195*, 120–125. [[CrossRef](#)]
54. Zhang, S.T.; Liu, Y. Molecular-level mechanisms of quartz dissolution under neutral and alkaline conditions in the presence of electrolytes. *Geochem. J.* **2014**, *48*, 189–205. [[CrossRef](#)]
55. Yu, K.H.; Cao, Y.C.; Qiu, L.W.; Sun, P.P.; Su, Y.G. Brine evolution of ancient lake and mechanism of carbonate minerals during the sedimentation of Early Permian Fengcheng Formation in Mahu Depression, Junggar Basin, China. *Nat. Gas Geosci.* **2016**, *27*, 1248–1263.
56. Zhao, Y.; Guo, P.; Lu, Z.Y.; Zheng, R.C.; Chang, H.L.; Wang, G.Z.; Wei, Y.; Wen, H.G. Genesis of Reedmergnerite in the Lower Permian Fengcheng Formation of the Junggar Basin, NE China. *Acta Sedimentol. Sin.* **2020**, *38*, 966–979.
57. Zhang, H.; Cheng, L.; Fan, H.T. Formation overpressure and its influence on physical properties in Mahu sag, Junggar Basin. *Prog. Geophys.* **2022**, *37*, 1223–1227.
58. Zhang, S.T.; Liu, Y. Progress Review of Quartz Dissolution Models. *Bull. Miner. Petrol. Geochem.* **2009**, *28*, 294–300.
59. Tian, X.R.; Zhang, Y.Y.; Zhuo, Q.G.; Yu, Z.C.; Guo, Z.J. Tight oil charging characteristics of the Lower Permian Fengcheng Formation in Mahu sag, Junggar Basin: Evidence from fluid in alkaline minerals. *Acta Pet. Sin.* **2019**, *40*, 646–659.
60. Rao, S.; Zhu, Y.K.; Hu, S.B.; Wang, Q. The Thermal History of Junggar Basin: Constraints on the Tectonic Attribute of the Early-Middle Permian Basin. *Acta Geol. Sin.* **2018**, *92*, 1176–1195.
61. Zhu, S.F.; Zhu, X.M.; Wu, D.; Liu, Y.H.; Li, P.P.; Jiang, S.X.; Liu, X.C. Alteration of volcanics and its controlling factors in the Lower Permian reservoirs at northwestern margin of Junggar Basin. *Oil Gas Geol.* **2014**, *35*, 77–85.
62. Guo, M.Z.; Shou, J.F.; Xu, Y.; Guo, H.J.; Zou, Z.W.; Han, S.H. Distribution and controlling factors of Permian zeolite cements in Zhongguai—Northwest margin of Junggar Basin. *Acta Pet. Sin.* **2016**, *37*, 695–705.
63. Chipera, S.J.; Goff, F.; Goff, C.J.; Fittipaldo, M. Zeolitization of intracaldera sediments and rhyolitic rocks in the 1.25 Ma lake of Valles caldera, New Mexico, USA. *J. Volcanol. Geotherm. Res.* **2008**, *178*, 317–330. [[CrossRef](#)]
64. Zhu, S.F.; Zhu, X.M.; Liu, X.C.; Li, C.; Wang, X.X.; Tan, M.X.; Geng, M.Y.; Li, Y.P. Alteration products of volcanic materials and their influence on reservoir space in hydrocarbon reservoirs: Evidence from Lower Permian strata in Ke-Xia region, Junggar Basin. *Acta Pet. Sin.* **2014**, *35*, 276–285.
65. Zhu, S.F.; Zhu, X.M.; Wang, X.L.; Liu, Z.Y. Zeolite diagenesis and its control on petroleum reservoir quality of Permian in northwestern margin of Junggar Basin, China. *Sci. China Earth Sci.* **2012**, *55*, 386–396. [[CrossRef](#)]
66. Chang, H.L.; Zheng, R.C.; Guo, C.L.; Wen, H.G. Characteristics of Rare Earth Elements of Exhalative Rock in Fengcheng Formation, Northwestern Margin of Jungger Basin. *Geol. Rev.* **2016**, *62*, 550–568.
67. Zhu, S.F.; Zhu, X.M.; Niu, H.P.; Han, X.F.; Zhang, Y.Q. Genetic Mechanism of Dolomitization in Fengcheng Formation in the Wu-Xia area of Junggar Basin, China. *Acta Geol. Sin.-Engl. Ed.* **2012**, *86*, 447–461.
68. Guo, P.; Wen, H.G.; Gibert, L.; Jin, J.; Jiang, Y.Q.; Wang, G.Z. Controlling factors of high quality hydrocarbon source rocks developed in lacustrine shallow-water zone of the Junggar Basin, northwestern China. *AAPG Bull.* **2021**, *105*, 2063–2092. [[CrossRef](#)]
69. Guo, P.; Wen, H.; Gibert, L.; Jin, J.; Wang, J.; Lei, H. Deposition and diagenesis of the Early Permian volcanic-related alkaline playa-lake dolomitic shales, NW Junggar Basin, NW China. *Mar. Pet. Geol.* **2020**, *123*, 104780. [[CrossRef](#)]
70. Broxton, D.E. Chemical changes associated with zeolitization of the tuffaceous beds of Calico Hills, Yucca Mountain, Nevada, USA. *Proc. Int. Symp. Water-Rock Interact.* **1992**, *7*, 699–703.
71. Lijima, A. Zeolites in petroleum and natural gas reservoirs. *Rev. Mineral. Geochem.* **2001**, *45*, 347–402.

72. Jia, B.; Wen, H.G.; Li, Y.B.; Liu, Y.P.; Wang, T. Fluid inclusions in the salt minerals from the Permian Fengcheng Formation in the Urho region, Junggar Basin, Xinjiang. *Sediment. Geol. Tethyan Geol.* **2015**, *35*, 33–42.
73. Lovley, D.R.; Holmes, D.E.; Nevin, K.P. Dissimilatory Fe(III) and Mn(IV) reduction. *Adv. Microb. Physiol.* **2004**, *49*, 219–286.
74. Jin, Q.; Wang, J.; Song, G.Q.; Wang, L.; Lin, L.M.; Bai, S.P. Interaction between source rock and evaporite: A case study of natural gas generation in the northern dongying depression. *Chin. J. Geochem.* **2010**, *29*, 75–81. [[CrossRef](#)]
75. Zhi, D.M.; Tang, Y.; Zheng, M.L.; Xu, Y.; Cao, J.; Ding, J.; Zhao, C.Y. Geological characteristics and accumulation controlling factors of shale reservoirs in Fengcheng Formation, Mahu sag, Junggar Basin. *China Pet. Explor.* **2019**, *24*, 615–623.
76. Hips, K.; Haas, J.; Poros, Z.; Kele, S.; Budai, T. Dolomitization of Triassic microbial mat deposits (Hungary): Origin of microcrystalline dolomite. *Sediment. Geol.* **2015**, *318*, 113–129. [[CrossRef](#)]
77. Cao, J.; Zhang, Y.J.; Hu, W.X.; Yao, S.P.; Wang, X.L.; Zhang, Y.Q.; Tang, Y. The Permian hybrid petroleum system in the northwest margin of the Junggar Basin, northwest China. *Mar. Pet. Geol.* **2005**, *22*, 331–349. [[CrossRef](#)]

**Disclaimer/Publisher’s Note:** The statements, opinions and data contained in all publications are solely those of the individual author(s) and contributor(s) and not of MDPI and/or the editor(s). MDPI and/or the editor(s) disclaim responsibility for any injury to people or property resulting from any ideas, methods, instructions or products referred to in the content.